

Luděk Beneš; Karel Kozel; Ivo Sládek

Numerical modeling of flow and pollution dispersion over real topography

In: Jan Chleboun and Karel Segeth and Tomáš Vejchodský (eds.): Programs and Algorithms of Numerical Mathematics, Proceedings of Seminar. Prague, May 28-31, 2006. Institute of Mathematics AS CR, Prague, 2006. pp. 9–15.

Persistent URL: <http://dml.cz/dmlcz/702812>

Terms of use:

© Institute of Mathematics AS CR, 2006

Institute of Mathematics of the Czech Academy of Sciences provides access to digitized documents strictly for personal use. Each copy of any part of this document must contain these *Terms of use*.



This document has been digitized, optimized for electronic delivery and stamped with digital signature within the project *DML-CZ: The Czech Digital Mathematics Library*
<http://dml.cz>

NUMERICAL MODELING OF FLOW AND POLLUTION DISPERSION OVER REAL TOPOGRAPHY*

Luděk Beneš, Karel Kozel, Ivo Sládek

1. Introduction

The Atmospheric Boundary Layer (ABL) is the lowest part of the atmosphere. Its thickness usually ranges from several hundred meters to approximately two kilometers. The air pollution resulting from rapid industrialization has become a serious environmental problem mainly in the North Bohemia region. In this contribution, the influence of several types of obstacles on dustiness of coal depot in open coal mine was numerically modeled.

2. Mathematical models

In our computations, the flow in ABL is assumed to be viscous, steady, incompressible, turbulent and indifferently stratified. Two different mathematical and numerical methods have been used for numerical simulations.

• The full RANS model

The first model is based on Reynolds Averaged Navier–Stokes equations. The governing equations are considered in the conservative, non-dimensional, and vector form:

$$W_t + F_x + G_y + H_z = (KR)_x + (KS)_y + (KT)_z + f_v, \quad (1)$$

where $F = (u, u^2+p, uv, uw, uC)^T$, $G = (v, vu, v^2+p, vw, vC)^T$, $H = (w, wu, wv, w^2 + p, wC)^T$, $R = (0, u_x, v_x, w_x, C_x/\sigma_C)^T$, $S = (0, u_y, v_y, w_y, C_y/\sigma_C)^T$, $T = (0, u_z, v_z, w_z, C_z/\sigma_C)^T$. $W = (p/\beta^2, u, v, w, C)^T$ stands for the vector of unknown variables the pressure, three velocity components $V = (u, v, w)^T$, and the concentration of passive pollutant, respectively. Further f_v denotes the volume force, σ_C is the turbulent Prandtl's number, β artificial compressibility coefficient and finally K represents the turbulent diffusion coefficient, see equation (5). The artificial compressibility method is used for the numerical solution of this model.

• Boussinesq equations

The NS equations are simplified by the so called Boussinesq approximation. The instantaneous values of the density, pressure and potential temperature can be decomposed into two parts: the large synoptic scale part denoted by subscript $_0$ and

*The financial support for the presented project is partly provided by the Research Plan MSM No. 6840770003 and GAČR 205/06/0727.

its perturbation denoted by $''$. Then the governing equations for the neutrally stratified flow can be rewritten in the following form

$$(\rho_0 u)_x + (\rho_0 v)_y + (\rho_0 w)_z = 0, \quad (2)$$

$$V_t + uV_x + vV_y + wV_z = -\frac{\nabla p''}{\rho_0} + \frac{1}{\rho_0} \left\{ [\rho_0 K V_x]_x + [\rho_0 K V_y]_y + [\rho_0 K V_z]_z \right\} + f_v. \quad (3)$$

The transport equations for the passive pollutant C is

$$C_t + uC_x + vC_y + wC_z = \left[\left(\frac{K}{\sigma_C} C_x \right)_x + \left(\frac{K}{\sigma_C} C_y \right)_y + \left(\frac{K}{\sigma_C} C_z \right)_z \right]. \quad (4)$$

2.1. Turbulence model

Closure of both systems of governing equations (1) and (2)–(4) is achieved by a simple algebraic turbulence model designed for ABL flow. The model is based on the Bousinesq hypothesis. The diffusion coefficient K has the following form in the dimensional case

$$K = \nu + \nu_T, \quad \nu_T = l^2 \sqrt{(u_z)^2 + (v_z)^2}, \quad (5)$$

where ν_T and ν are the turbulent and laminar viscosities. The mixing length l is according to Blackadar computed from

$$l = \frac{\kappa(z + z_0)}{1 + \kappa(z + z_0)/l_\infty}, \quad l_\infty = \frac{27 |V_g| 10^{-5}}{\lambda}, \quad (6)$$

where κ is the von Karman constant, λ denotes the Coriolis parameter, z_0 the roughness length, l_∞ denotes the mixing length for $z \rightarrow \infty$ and V_g is the geostrophic wind velocity at the upper boundary of the domain.

3. Numerical methods

We have solved the governing systems of equations with stationary boundary conditions and we suppose that we obtain the expected steady-state solution for $t \rightarrow \infty$. Structured non-orthogonal grids made of hexahedral (in 3D case) and quadrilateral (in 2D case) control cells are used.

3.1. Finite volume method

The finite volume method (cell-centered type) together with the 3-stage explicit Runge–Kutta time integration scheme have been applied to solve equation (1). For discretization of viscous fluxes, a second octohedral mesh was used.

The numerical method is theoretically second order accurate in space and time on orthogonal grids. In addition, it must be stabilized by the artificial viscosity term of fourth order to remove spurious oscillations in the flow-field due to sharp gradients of computed quantities and also due to the central differences used for the space discretization of convective terms.

3.2. Finite difference method

A semi-implicit finite difference scheme has been used for the model (2)–(4). The special combination of different nonsymmetric space discretizations at time level n and $n + 1$ leads to the numerical scheme that is centered and second order both in space and time. In order to improve the convergence of this method for large Reynolds numbers the artificial viscosity terms either of the fourth or the second order are added. To discretize the governing system (2)–(4) we have constructed a non-orthogonal structured boundary–terrain fitted mesh.

3.3. Boundary conditions

Both models use the following boundary conditions.

- Inlet: $u = U_0(z/L)^\alpha$, $v = w = C = 0$, where L is vertical length of the domain and α is a power law exponent (we usually set $\alpha = 2/9$).
- Outlet: $u_x = v_x = w_x = C_x = 0$.
- Wall: the no-slip condition for the velocity components, $\partial C / \partial n = 0$.
- Top: $u = U_0$, $v = 0$, $\partial w / \partial z = \partial C / \partial z = 0$.
- Sides: periodic or non-periodic.

3.4. Validation of models

The first model (1) has been validated through the ERCOFTAC’s test-case of fully developed channel flow over 2D polynomial-shaped hill mounted on a flat plate. The Almeida’s experimental and the ERCOFTAC’s $k - \varepsilon$ reference numerical data have been used for the comparison, see [5].

The second model (2)–(4) has been validated on the experimental and reference numerical data obtained by G.H. Kim [6]. Boundary layer type of flow over the sinusoidal 2D-single-hills of different shapes has been tested [1].

The results from both validation studies has shown very good agreement with the target data.

4. Numerical results

This practical problem is related to the flow over a surface coal field located in the open coal mine in the North Bohemia. This numerical study is a continuation of the project we have been solving since 2001 in cooperation with Brown Coal Research Institute in Most. The major task was to design a safety obstacle close to a coal depot in order to decrease the level of pollutant concentrations in the down stream region which is inhabited. Several types of obstacles as solid wall, protective tree line, forest block and shelter belt were tested.

The influence of the forest blocks and the protective walls on the dustiness of the coal depot has been studied on the real topography of the coal depot.

The model of a real 3D relief was created on the basis of the topographic data obtained by the Brown Coal Research Institute in Most. The whole topography has been divided into two parts. The computational Domain 1, (see Figs. 1,2) is 800 m long, 480 m wide and the upper side is at 1000 m . The coal depot has dimensions

$80 \times 20 \text{ m}$ and it is situated at the origin. For better resolution of the flow field close to the depot, the second Domain 2 $400 \times 240 \text{ m}$ was imbedded (see Fig. 2). The data obtained on Domain 1 were used as the boundary and initial conditions for the computations on Domain 2.

Both domains have been discretized using $100 \times 60 \times 40$ mesh cells, so the horizontal resolution is 8 m on Domain 1 and 4 m on Domain 2. Both grids are significantly thickened close to the ground with $\Delta_{z_{\min}} \approx 0.6 \text{ m}$. Two variants were computed in 3D: basic (without protective obstacles) and with two forest blocks situated before and behind the coal depot.

The **solid wall** was simulated by the column of a few cells. All the velocity components have been set to zero in all of these cells. For the **forest block**, the force vector \vec{f}_v includes the specific aerodynamic force corresponding to the drag induced by the vegetation, i.e.

$$\vec{f}_v = (-r_h|V|u, -r_h|V|v, -r_h|V|w)^T. \quad (7)$$

Here the $r_h(z)$ denotes the total resistance parameter. The vertical profile of this parameter has been set-up in the following way:

$$r_h(z) = \begin{cases} rz/(0.75h) & \text{for } 0 \leq z/h \leq 0.75, \\ r(1 - z/h)/(1 - 0.75) & \text{for } 0.75 \leq z/h \leq 1.0, \end{cases} \quad (8)$$

where the drag coefficient value r is given a priori.

The other parameters are: mean free stream velocity $U = 10 \text{ m/s}$, roughness parameter $z_0 = 0.1 \text{ m}$ and power law exponent $2/9$ are used for the inlet velocity profile (Domain 1). The forest blocks are 10 m high with the drag coefficient $r = 0.19$. The wall is 5 m high.

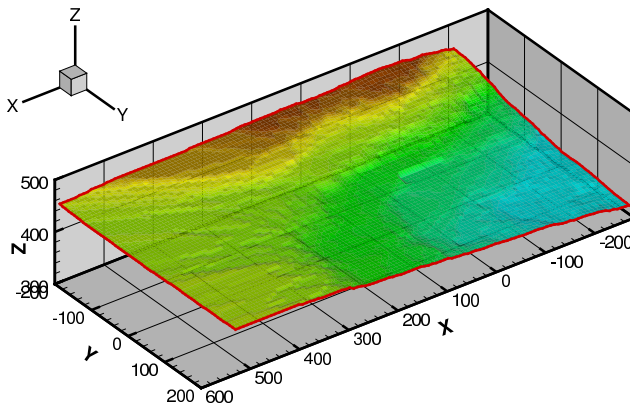


Fig. 1: Topography of the mine–Domain 1.

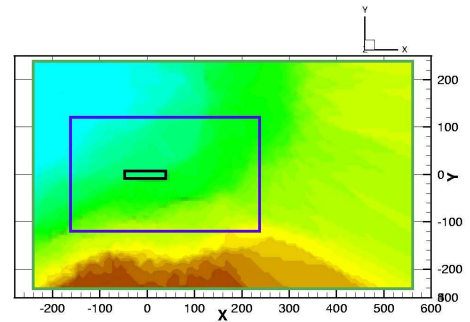


Fig. 2: Computational Domain 1, Domain 2 (larger rectangle), coal depot (smaller rectangle).

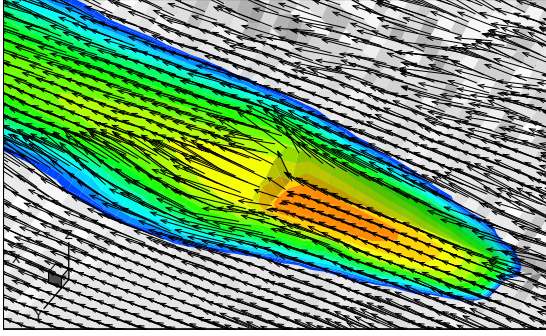


Fig. 3: *Velocity vectors close to the coal depot – basic situation. Colored by the concentration.*

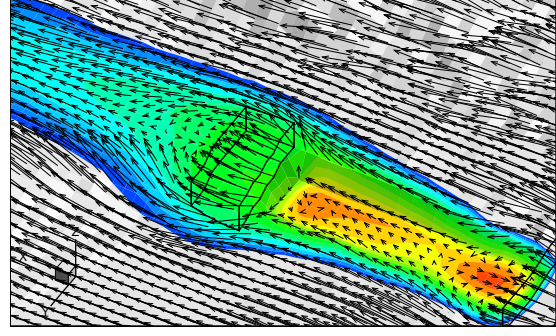


Fig. 4: *Velocity vectors close to the coal depot – situation with two forests. Colored by the concentration.*

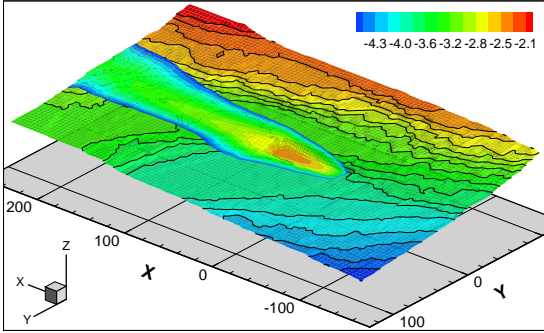


Fig. 5: *Concentration of the pollution in the logarithmic scale completed by altitude – basic situation.*

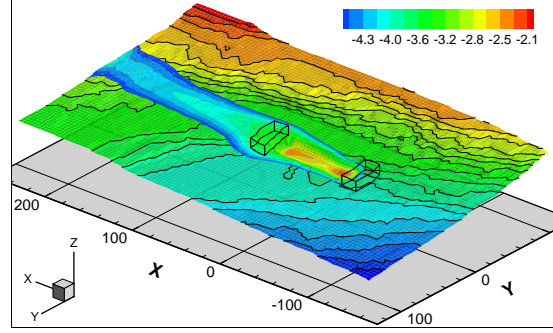


Fig. 6: *Concentration of the pollution in the logarithmic scale completed by altitude – situation with two forests.*

In Figs. 3 and 4 and Figs. 5 and 6 we can see the comparison of the flow field and the pollution dispersion in two different cases – basic and with two forests before and behind the coal depot. From these figures one can see considerable reduction of the dustiness in the second case. It is due to the significant deceleration of the flow behind the forest on the area of coal depot.

The majority of variants has been tested in 2D only. From Domain 1 the 2D middle cut ($y = 0$) was chosen. This cut was discretized by 800×40 cells (horizontal resolution 1 m), vertical distribution is the same as in 3D. Also the other computational parameters are the same as in 3D.

The seven different positions and combinations of walls and forests were computed in 2D case: basic – without protective obstacles (zak), with the forest block before (a) behind (b) and on both sides (ab) of the depot, and with the wall before (fa) behind (fb) and on both sides (fab).

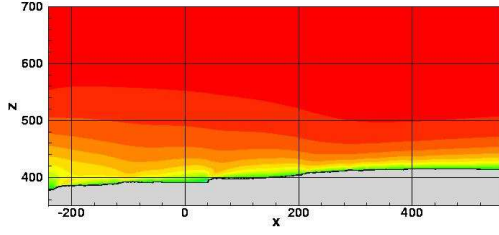


Fig. 7: *Basic variant – velocity component u .*

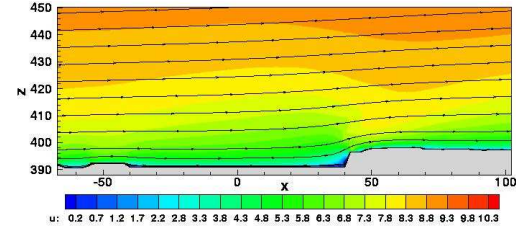


Fig. 8: *Basic var. – velocity component u with streamlines close to the coal depot.*

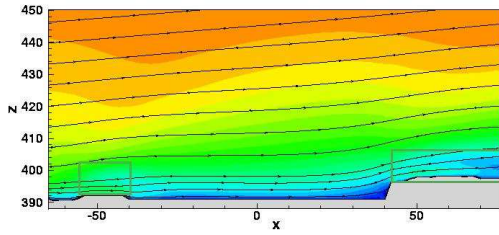


Fig. 9: *Variant ab – velocity component u with streamlines close to the c.d.*

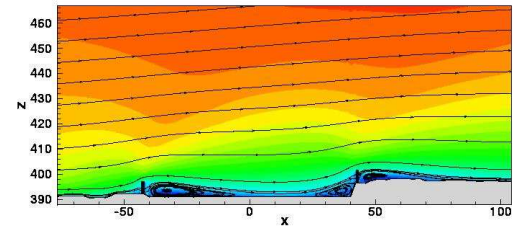


Fig. 10: *Variant fab – velocity component u with streamlines close to the c.d.*

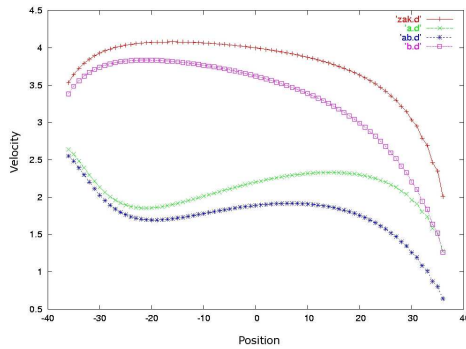


Fig. 11: *The longitudinal distribution of near-ground velocity in case of forest.*

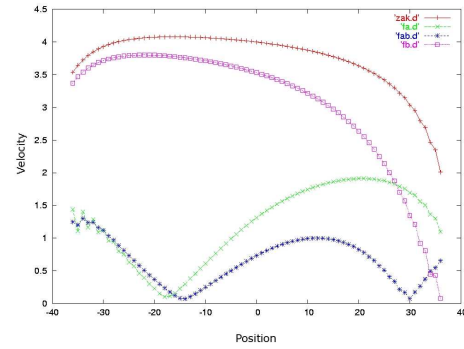


Fig. 12: *The longitudinal distribution of near-ground velocity in case of walls.*

Figs. 7–10 show the comparison of the basic variant with two different cases in 2D: with forest on both sides (ab) of the coal depot and also with a wall on both sides (fab). In Fig. 10 large recirculation zones behind the walls are shown. In contrast, the flow going through the forest is decelerated smoothly without recirculation, Fig. 9.

In our model, the source intensity is proportional to the vertical velocity gradient, and the mesh is uniform on the coal depot. Therefore the local source intensity is proportional to the ground velocity.

Fig. 11 and Fig. 12 shows the longitudinal distribution of near ground velocity for an obstacle of type forest block (left) and walls (right).

References

- [1] L. Beneš, T. Bodnár, Ph. Fraunié, K. Kozel: *Numerical modelling of pollution dispersion in complex terrain*. In: G. Latini, C.A. Brebbia (eds), Air Pollution IX., Southampton, WIT Press, 2001, 85–94.
- [2] T. Bodnár, Ph. Fraunié, K. Kozel, I. Sládek: *Numerical simulation of complex atmospheric boundary layer problems*. In: J.M. Redondo (ed.), ERCOFTAC Bulletin No. 60, March 2004, 5–12.
- [3] T. Bodnár, I. Sládek, E. Gulíková: *Numerical simulation of wind flow in the vicinity of forest block*. In: S.N. Atluri (ed.), Advances in Computational & Experimental Engineering & Sciences. Forsyth, Tech Science Press, 2004, 554–559.
- [4] E. Gulíková, T. Bodnár, V. Píša: *Improvement of numerical models for solution of dust air pollution*. In: J. Příhoda, K. Kozel (eds.), Colloquium FLUID DYNAMICS 2006, Prague, IT ASCR, 2005, 63–66.
- [5] G.P. Almeida, D.F.G. Durao, M.V. Heitor: *Wake flows behind two dimensional model hills*. Exp. Thermal and Fluid Science **7**, 1992, 87–101.
- [6] G.H. Kim, M.Ch. Lee, C.H. Lim, H.N. Kyong: *An experimental and numerical study on the flow over two-dimensional hills*. Journal of Wind Eng. and Industrial Aerodynamics **66**, 1997, 17–33.